Multidetector Scattering as a Probe of Local Structure in Disordered Phases

Noel A. Clark
Department of Physics, University of Colorado, Boulder, Colorado 80309

and

Bruce J. Ackerson
Department of Physics, Oklahoma State University, Stillwater, Oklahoma 74074

and

Alan J. Hurd
Department of Physics, Brandeis University, Waltham, Massachusetts 02154
(Received 24 February 1983)

The local translational structure of a two-dimensional colloidal liquid is observed by use of cross correlation of the intensity fluctuations of light scattered by the liquid through two different wave vectors. The utility of multidetector scattering in probing multipoint correlations in disordered phases is thereby demonstrated unambiguously.

PACS numbers: 61.25.Hq, 68.90.+g, 78.35.+c

The study of static and dynamic pair correlation functions by scattering techniques has been perhaps the single most useful tool in the effort to characterize structure in disordered phases.[1] As useful as pair correlations have been, however, the information they provide is limited. For example, the static pair correlation function of a simple fluid, $g(r)$, although giving the density of particles about one at the origin, provides no direct information on local structure, i.e., what *arrangements* of particles are to be typically found. This information is contained in the relative locations of three or more particles, and is characterized by a hierarchy of multipoint correlation functions. These functions, unfortunately, have proved virtually inaccessible to experimental study, although, following the pioneering theory of Cantrell,[2] multidetector light scattering has been proposed to probe them.[3-5]

In this Letter we demonstrate the use of multidetector light scattering to provide information on local structure in condensed phases beyond that obtainable from pair correlations. We exhibit the local translational structure of a two-dimensional colloidal liquid using cross-correlation intensity-fluctuation spectroscopy of light scattered through two different wave vectors. Our approach is basically different from previous approaches[2-5] in that we specifically limit the scattering volume size and take advantage of the resulting non-Gaussian scattered-field statistics.[6,7]

The experimental geometry is shown in Fig. 1(a). The sample is a single layer of polystyrene spheres in aqueous suspension trapped between a pair of flat quartz plates. The particles (diameter, 0.234 μm), charged by acidic surface groups, interact with each other and the quartz plates via an electrostatic repulsion that is screened by H^+ counterions in solution. The gap between the plates is wedge shaped, with the monolayer of spheres exhibiting two-dimensional (2D) crystal, liquid, and gaseous phases successively as the plate spacing decreases. The crystal and liquid phases were separated by a well-defined interface line, with the liquid density smoothly decreasing to the gas phase. Ar^+ laser light ($2\pi/K = 4880$ Å), focused to a Gaussian beam waist of diameter $d = 5.3$ μm, was incident normal to the sample plane.

Figure 1(b) shows the scattered intensity distribution, $I(\vec{K})$, from the crystalline phase obtained with the beam waist in the sample plane. The pattern of six diffraction-limited spots hexagonally arranged on a circle in K space (radius, K_{10}) indicates a single-crystal region of the sample having particles distributed on a 2D hexagonal lattice. The particle spacing (lattice parameter, a) is 0.9 μm, so that $\simeq 25$ particles are being illuminated. Figure 1(c) shows the Debye-Scherrer (DS) ring (radius, K_{DS}) obtained in the liquid phase with the beam waist of the incident light displaced from the sample plane so that a sample area of relatively large dimension, $d \simeq 50$ μm diam, is illuminated. The DS ring width, ΔK_{DS}, is determined primarily by the range of local translational order, with some contribution from the K spread of the incident light. In Fig. 1(c), because $1/d$ is small compared with ΔK_{DS}, $I(\vec{K})$ exhibits many speckles or coherence areas, of

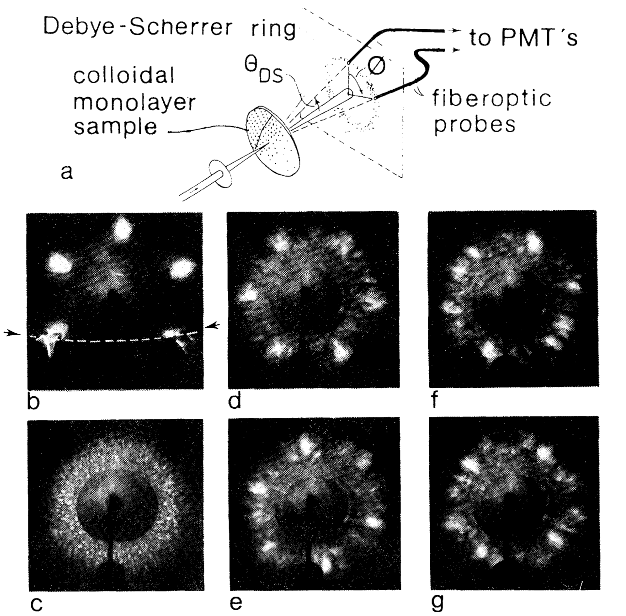

FIG. 1. (a) Schematic of the experiment. The sample was a monolayer to submonolayer of charged polymer spheres in aqueous colloidal suspension, contained in a thin, wedge-shaped gap between flat quartz plates. In the thickest part of the sample ($t \simeq 10$ μm) the monolayer was crystalline, 2D hcp, which was separated by a well-defined interface from the liquid region. The liquid density gradually decreased upon moving to the thinner parts of the sample. Measurements were made in the liquid phase, away from the immediate vicinity of the liquid-crystal interface. (b)–(g) Photographs of typically observed scattered light distributions obtained from video records of the scattered intensity on a screen parallel to the sample plane [dashed parallelogram in (a)]. A stop intercepted the incident laser beam, which is directed normal to the page toward the reader through the center of each photo: (b) Scattering from a 5.3-μm-diam region (25 particles) of the 2D hcp crystalline phase, showing three of the six 2D-hcp spots on the radius K_{10}. The bottommost spots are blocked by the cell edge, indicated by the white dashed line and arrows. The beam waist is in the sample plane so that the Bragg spot size is diffraction limited, i.e., determined solely by the wave-vector distribution of the incident light. (c) Debye-Scherrer diffuse ring in the liquid phase, with the incident beam waist away from the sample plane, such that a $d \simeq 50$-μm-diam area is illuminated. The speckle size, K_{coh}, is comparable to $1/d$. The Debye-Scherrer ring radius, K_{DS}, in the liquid is identical with K_{10} in the crystal at the liquid-crystal interface line, and decreases as one moves further into the liquid phase. (d)–(g) Samples of the $I(\vec{K})$, averaged over a video-frame time ($\simeq 30$ ms), obtained in the liquid phase with $2\pi/K_{DS} = 0.87$ μm and $\simeq 25$ particles illuminated. Note the strong sixfold correlations and anticorrelations in a given sample. Samples (f) and (g) indicate in particular that $I(\vec{K}) \approx I(-\vec{K})$, the condition exactly satisfied at any given time for scattering by particles confined to a plane.

typical dimension $K_{coh} \simeq 1/d$. By reducing d the speckle size can be increased to become comparable in dimension to ΔK_{DS}, under which condition a dramatic change in the nature of the instantaneous scattered intensity distribution becomes visually evident [Figs. 1(d)–1(g)]. The scattering becomes characterized by the momentary appearance and disappearance of six-spot patterns reminiscent of the crystalline phase and having the same K_{10}. These fluctuating six-spot patterns appear with random orientation and persist for a few tens of milliseconds.

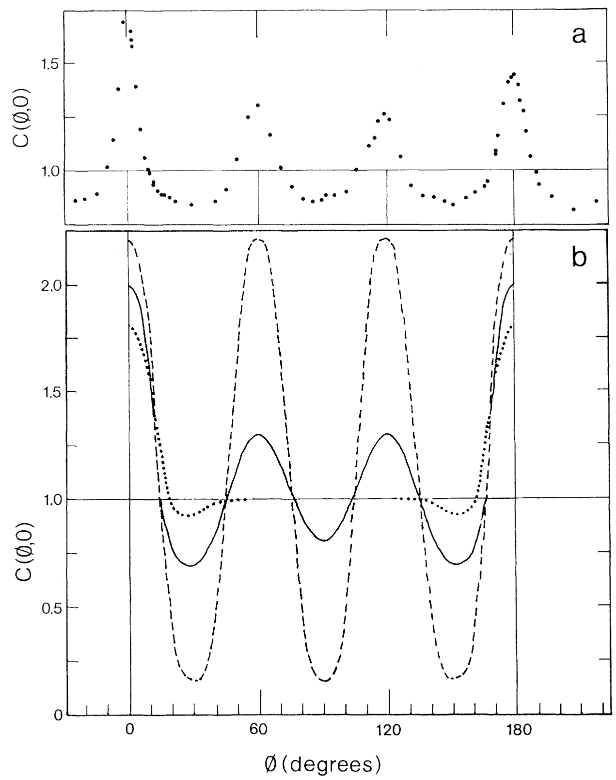

FIG. 2. (a) The measured normalized zero-time intensity cross-correlation function, $C(\varphi, 0)$, obtained in the 2D colloidal liquid. These data show strong positive correlation at $\varphi = 0°$, 60°, 120°, and 180°, displaying directly the 2D-hcp nature of the local liquid structure. If the condition $I(\vec{K}) = I(-\vec{K})$ were exactly satisfied the 0° and 180° peaks of $C(\varphi, 0)$ would have identical peak values. However $C(180°, 0)$ is smaller, most probably because of fluctuations involving displacements of the particles normal to the plane of the monolayer. (b) Theoretical $C(\varphi, 0)$ obtained from the rotating-fluctuating lattice model, discussed in the text, for a seven-particle cluster for various values of the parameter f, the rms relative displacement of nearest neighbors divided by the lattice parameter (dashed curve, $f = 0$; solid curve, $f = 0.2$; dotted curve, $f = 4$).

Under the conditions of Figs. 1(d)–1(g), namely that the region sampled in the liquid becomes comparable to the correlation area for translational ordering, it is evident that, at a given time, strong correlations and anticorrelations develop at different $\vec{K}$'s in the scattered field. In order to quantitatively characterize these correlations, light was collected at two regions in the scattered field, i.e., about two scattering vectors, $\vec{K}_1$ and $\vec{K}_2$, with use of a pair of 1-mm-diam fiber-optic bundles. Each of these directed the collected light to a separate photomultiplier and photon counting electronics, resulting in a pair of photopulse trains of count rates $n_1(t) \propto I(\vec{K}_1, t)$ and $n_2(t) \propto I(\vec{K}_2, t)$ which were fed into a digital cross correlator (Langley-Ford 1096). The fiber-optic probes were placed on the DS ring so that $K_1 = K_2 = K_{DS}$, and were separated by the angle φ about the ring center. In this Letter we present measurements of the normalized zero-time intensity cross-correlation function $C(\varphi, \tau = 0) \equiv \langle n_1(0) n_2(0)\rangle / \langle n\rangle^2$.

Figure 2(a) shows typical $C(\varphi, 0)$ data. As can be expected from Figs. 1(d)–1(g), this cross-correlation function shows strong positive peaks for $\varphi = 0°$, 60°, 120°, and 180° and anticorrelations at angles between these. Hence $C(\varphi, 0)$ displays directly that, at a given instant, the liquid is a mosaic of 2D hexagonally ordered regions.

The connection of $C(\varphi, 0)$ to liquid structure begins with the general form for the normalized intensity cross-correlation function in the single-scattering Born approximation:

$$C(\varphi, 0) = \langle \sum_{\substack{i,j\\l,m}} \epsilon_i \epsilon_j \epsilon_l \epsilon_m \exp[i\vec{K}_1 \cdot (\vec{r}_i - \vec{r}_j) + i\vec{K}_2 \cdot (\vec{r}_l - \vec{r}_m)]\rangle / S(\vec{K}_1) S(\vec{K}_2),$$

where $\epsilon_i = \epsilon(\vec{r}_i)$ and $S(\vec{K}) = \langle \sum \epsilon_i \epsilon_j \exp[i\vec{K}\cdot(\vec{r}_i - \vec{r}_j)]\rangle$. Plane wave fronts are assumed to illuminate the sample, with the field amplitude distribution, $\epsilon(\vec{r})$, defining the scattering volume.

To proceed further[8] we note the features of the measured $C(\varphi, 0)$ that the width of the peaks is approximately that of the diffraction-broadened crystal spots of Fig. 1(b), but that the 60° and 120° peaks are broader and of lower amplitude than the 0° and 180° peaks. A possible interpretation of this is that the local hexagonal structure of the liquid is dynamically distorted by vibrational fluctuations which at any given time may displace the diffraction spots from their locations in an ideal hexagonal reciprocal lattice, leading to a smearing of the 60° and 120° peaks. This suggests that the 2D colloidal fluid might be modeled by a two-dimensional polycrystalline solid with large vibrational fluctuations.[9] We therefore adopt a simplified model, ignoring number fluctuations and assuming that the scattering volume contains a uniformly illuminated hcp cluster of particles, taken to be part of an infinite 2D lattice which supports thermal vibrations as it adopts random orientations which are constant over the relevant vibration periods. Averages over lattice orientations, denoted by double angular brackets, neglect reorientation dynamics, in accord with our observations that these local structured regions come and go without significantly reorienting. Averages over lattice vibrations are denoted by $\langle \cdots \rangle_{\rm lv}$. The assumption that $g_{ij} = \langle\langle (\delta\vec{u}_i - \delta\vec{u}_j)^2\rangle_{\rm lv}$, the mean square relative displacement of a pair of particles (i,j), grows *linearly* with particle separation for separations less than d allows expression of $C(\varphi, 0)$ in terms of the g_{ij}:

$$\langle C(\varphi, 0)\rangle = S(K)^{-2} \sum_{\substack{i,j\\l,m}} \epsilon_i \epsilon_j \epsilon_l \epsilon_m J_0(\omega_{ijlm}) \exp\{-\tfrac{1}{2}[K_1^2 g_{ij} + K_2^2 g_{lm} + \vec{K}_1 \cdot \vec{K}_2 (g_{jl} + g_{im} - g_{il} - g_{jm})]\},$$

where

$$J_0(\omega_{ijlm}(\vec{K}_1, \vec{K}_2, \varphi)) = \langle\langle \exp[i\vec{K}_1 \cdot (\vec{r}_i - \vec{r}_j) + i\vec{K}_2 \cdot (\vec{r}_l - \vec{r}_m)]\rangle\rangle,$$

and $\vec{r}_i$ locates a particle in a randomly oriented perfect 2D-hcp lattice.

The resulting correlation functions, $C(\varphi, 0)$, for a 2D fluid with $K_1 = K_2 = K_{10} = K_{DS}$ are shown in Fig. 2(b), calculated for a seven-particle cluster for three values of $f = (g_{n,n+1})^{1/2}/a$, the rms relative vibration amplitude of nearest neighbors divided by particle spacing, a. For $f = 0$ we have the low-temperature limit: Particles are bound to their equilibrium positions and we obtain the cross-correlation function for a perfect hexagonal lattice executing random reorientational jumps. Note that for a small scattering volume the statistics of the scattered field are non-Gaussian so that $C(\varphi, 0)$ can have values larger than 2. For large f ($f = 0.4$) the particles move nearly independently in the scattering volume and there is no cross correlation: $C(\varphi, 0) = 1$, except in the homodyning limit, $\varphi \simeq 0°$ and 180°. Here $C(0, 0)$ approaches the ideal value,[7] $2 - 1/N$, for a finite number of particles. The width of the $\varphi = 0°$ peak for large f indicates the degree of diffraction broadening due to the finite sample volume size. For values of $f \approx 0.2$, the calculated $C(\varphi, 0)$ displays the main qualitative features of the experimental $C(\varphi, 0)$. There are peaks at $\varphi = 0°$, 60°, 120°, and 180° due to the basic lattice structure, with suppression of the 60° and 120° peaks because of the lattice vibrations which locally destroy the perfect translational lattice symmetry. The difference between the data and the model is due primarily to the small number of particles illuminated in the model, 7, vs 25 in the experiment. As d, and therefore the number of illuminated particles, N, increases, the peaks in $C(\varphi, 0)$ will narrow and grow in amplitude as long as the correlation length for local translational ordering, ξ, is larger than d. For $\xi < d$, the peaks will decrease in amplitude as long as d increases, but will never completely disappear. Model calculations for various N are currently underway.

Obvious extensions of these initial studies are to the space and time dependence of local structural correlation in 2D and 3D colloids. Finally, we suggest that such multidetector scattering techniques can be usefully applied in synchrotron x-ray studies of atomic and molecular systems, as it appears feasible that x-ray focusing technology permitting the requisite illumination of sufficiently small scattering volumes will soon be available.

We are indebted to D. H. Van Winkle for assistance with this experiment. This work was supported by National Science Foundation Solid State Chemistry Grant No. DMR 79-20169, Low Temperature Physics Grant No. DMR 82-06472, and Low Temperature Physics Grant No. DMR 81-16119.

[1]C. A. Croxton, *Liquid State Physics* (Cambridge Univ. Press, Cambridge, England, 1974); J. P. Hansen and I. R. McDonald, *Theory of Simple Liquids* (Academic, New York, 1976).

[2]C. D. Cantrell, Ph.D. thesis, Princeton University, 1968 (unpublished).

[3]J. Swift, Ann. Phys. (N.Y.) 75, 1 (1973).

[4]G. D. J. Phillies, Mol. Phys. 32, 1695 (1976).

[5]G. D. J. Phillies, J. Chem. Phys. 72, 6123 (1980); Z. Kam, Macromolecules 10, 927 (1977).

[6]W. G. Griffin and P. N. Pusey, Phys. Rev. Lett. 43, 1100 (1979).

[7]P. N. Pusey, in *Photon Correlation Spectroscopy and Velocimetry*, edited by H. Z. Cummins and E. R. Pike (Plenum, New York, 1977).

[8]We defer the discussion of $C(\varphi, \tau)$ in terms of multiparticle correlation functions; B. J. Ackerson and N. A. Clark, to be published.

[9]F. H. Stillinger and T. A. Weber, Phys. Rev. A 25, 978 (1982).

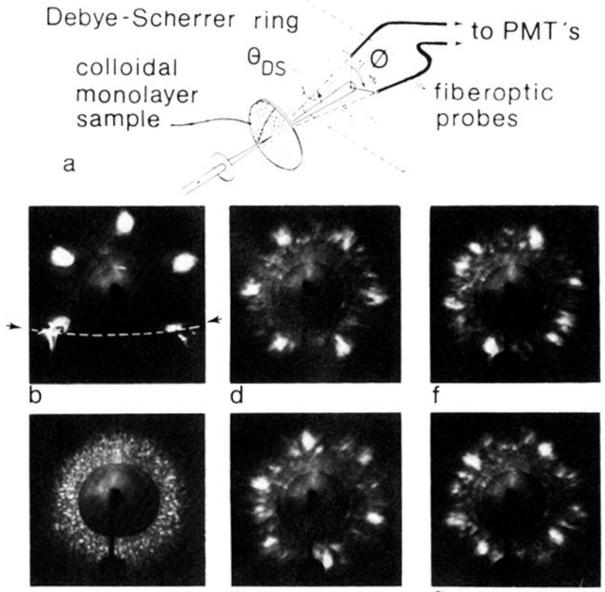

FIG. 1. (a) Schematic of the experiment. The sample was a monolayer to submonolayer of charged polymer spheres in aqueous colloidal suspension, contained in a thin, wedge-shaped gap between flat quartz plates. In the thickest part of the sample ($t \simeq 10$ μm) the monolayer was crystalline, 2D hcp, which was separated by a well-defined interface from the liquid region. The liquid density gradually decreased upon moving to the thinner parts of the sample. Measurements were made in the liquid phase, away from the immediate vicinity of the liquid-crystal interface. (b)–(g) Photographs of typically observed scattered light distributions obtained from video records of the scattered intensity on a screen parallel to the sample plane [dashed parallelogram in (a)]. A stop intercepted the incident laser beam, which is directed normal to the page toward the reader through the center of each photo: (b) Scattering from a 5.3-μm-diam region (25 particles) of the 2D hcp crystalline phase, showing three of the six 2D-hcp spots on the radius K_{10}. The bottommost spots are blocked by the cell edge, indicated by the white dashed line and arrows. The beam waist is in the sample plane so that the Bragg spot size is diffraction limited, i.e., determined solely by the wave-vector distribution of the incident light. (c) Debye-Scherrer diffuse ring in the liquid phase, with the incident beam waist away from the sample plane, such that a $d \simeq 50$-μm-diam area is illuminated. The speckle size, K_{coh}, is comparable to $1/d$. The Debye-Scherrer ring radius, K_{DS}, in the liquid is identical with K_{10} in the crystal at the liquid-crystal interface line, and decreases as one moves further into the liquid phase. (d)–(g) Samples of the $I(\vec{K})$, averaged over a video-frame time ($\simeq 30$ ms), obtained in the liquid phase with $2\pi/K_{DS} = 0.87$ μm and $\simeq 25$ particles illuminated. Note the strong sixfold correlations and anticorrelations in a given sample. Samples (f) and (g) indicate in particular that $I(\vec{K}) \approx I(-\vec{K})$, the condition exactly satisfied at any given time for scattering by particles confined to a plane.